Field Strength and Frequency-Dependent Effects of Pulsed Electric Fields on Soilborne Nematodes, Pathogens, and Weeds

Tatiana Benedeti
Oregon State University
Pamela Medeiros dos Santos
Oregon State University
Inga A. Zasada
Oregon State University
Jerry E. Weiland
Horticultural Crops Research Laboratory
Jason Crisp
Lisi Global
Marcelo L. Moretti
marcelo.moretti@oregonstate.edu

Oregon State University

Article

Keywords: Verticillium dahliae, Phytophthora cinnamomi, Phytophthora plurivora, Meloidogyne chitwoodi, Pratylenchus neglectus, Digitaria sanguinalis, Echinochloa crus-galli, Cyperus esculentus

Posted Date: April 6th, 2026

DOI: https://doi.org/10.21203/rs.3.rs-9203942/v1

Additional Declarations: Competing interest reported. The author Jason Crisp is the Chief Executive Officer of Lisi Global Inc., which develops pulsed electric field technology used in this study. The remaining authors declare no competing interests.

Version of Record: A version of this preprint was published at Scientific Reports on June 8th, 2026. See the published version at https://doi.org/10.1038/s41598-026-56820-y.

Abstract

Pulsed electric field (PEF) technology is a non-chemical approach with potential to control soilborne agricultural pests. PEF disrupts cellular membranes through short, high-energy electrical pulses. Treatment efficacy depends on electric field strength, pulse frequency, and applicator design. In this study, two soil-applied PEF applicators, vertical pins (VP) and parallel plates (PP), were evaluated for suppression of weeds, plant-parasitic nematodes, and soilborne pathogens. Numerical simulations showed that the PP configuration generated a more uniform electric field distribution than the VP design. Consistent with these predictions, the PP applicator provided greater biological suppression across target organisms. *Cyperus esculentus* biomass declined progressively with increasing energy density and was substantially reduced at ≥ 100 J cm^{-3}. The PP applicator also reduced *Meloidogyne chitwoodi* second-stage juveniles by up to 100% at 25 J cm^{-3} and pulse frequencies above 60 Hz. Populations of *Pratylenchus neglectus* and *M. chitwoodi* were reduced by more than 98% at 400 V mm^{-1}. Overall, nematodes and soilborne pathogens were suppressed at substantially lower energy densities (~ 25 J cm^{-3}) than weed propagules, which generally required ≥ 100–200 J cm^{-3} for effective biomass suppression. Weed responses were species dependent: biomass of *C. esculentus* and *Digitaria sanguinalis* declined at 100–200 J cm^{-3}, whereas *Echinochloa crus-galli* required higher energy inputs for control. Soilborne pathogens also differed in susceptibility, with *Phytophthora cinnamomi* and *P. plurivora* reduced by 94% at moderate field strengths (100–200 V mm^{-1}), *while* and *Verticillium dahliae* was suppressed by up to 97% at 200–400 V mm^{-1} and 80 Hz. Overall, nematodes and soilborne pathogens were suppressed at substantially lower energy densities (~ 25 J cm^{-3}) than weed propagules, which generally required ≥ 100–200 J cm^{-3} for effective biomass suppression. These results demonstrate that PEF can effectively suppress multiple soilborne pests; Additionally, the results highlight the importance of applicator design and electrical parameters in determining treatment efficacy, supporting the potential of PEF as a scalable and sustainable soil disinfestation technology.

Introduction

Soil disinfestation studies were conducted for one year to investigate the potential of PEF to reduce the significant economic and environmental losses caused by soilborne pathogens, weeds, parasitic plants, and arthropods[1]. Many alternative chemical, biological, and physical approaches have been tested as replacements for traditional chemical fumigants[2]. Pulsed electrical field (PEF) technology is an emerging strategy for agricultural pest management. PEF has been used in soil electrokinetic remediation[3], in the food processing industry, and in genetic engineering to inactivate bacteria, fungi, and yeasts[4,5]. More recently, it has demonstrated potential to control soilborne plant pathogens and plant-parasitic nematodes[6].

Pulsed electric field delivers short, high-voltage electrical pulses of micro- to millisecond duration, creating intense electric gradients across cell membranes. When the induced transmembrane potential exceeds a critical threshold, structural rearrangements occur within the lipid bilayer, leading to pore

formation[7,8]. The reversibility or irreversibility of the electroporation process depends on the electric gradient (field strength), pulse intensity, duration, number, and total energy input[9]. For example, PEF applied at an energy density of 25 J cm^{-3} to soil reduced *Meloidogyne hapla* egg viability, whereas an application of 70 J cm^{-3} reduced *Globodera ellingtonae* egg hatch by 85%[6]. At the same energy density, *Phytophthora cinnamomi* survival was reduced to nondetectable levels, while *Verticillium dahliae* survival was reduced by 73%[6].

The electric field is established between at least two electrodes of opposite polarities, separated by a defined physical distance. Field strength is calculated as applied voltage divided by electrode spacing. Electrode arrangement, geometry, spacing, surface area, and material strongly influence current density distribution, energy delivery, and treatment uniformity[10,11]. Nonuniform energy distribution within the treatment zone has been reported to reduce the effectiveness of PEF applications in the food industry[12]. As PEF delivery systems continue to improve, further research is needed to assess new PEF configurations to manage soilborne pests. The present study evaluated a newly developed parallel plate PEF applicator and compared its performance with a previously studied vertical pin configuration for the control of plant-parasitic nematodes, soilborne pathogens, and weeds, while accounting for field strength and field strength.

Results

• Applicator comparison

Two PEF applicator configurations, vertical pins (VP) and parallel plates (PP), were evaluated to determine how electrode geometry influenced electric field gradients and biological efficacy (Fig. 1). Numerical simulations of the electric potential distribution revealed clear differences in energy distribution between electrode configurations (Fig. 2). In the VP configuration, electric potential gradients were highly localized around the electrode tips, producing strong electric fields near the electrode-soil interface that rapidly dissipated with distance. In contrast, the PP configuration generated a more uniform electric field distribution across the treated soil volume, resulting in a broader exposure to similar electric field intensities. As the applied electric field increased from 50 to 400 V mm^{-1}, the magnitude of the electric potential increased proportionally in both configurations; however, spatial heterogeneity remained substantially greater in VP geometry. These differences reflect the contrasting electrode–soil interface characteristics of the two applicators. The PP applicator had a larger electrode surface area relative to the treated soil volume (A/V = 27.0 m^{-1}) compared with the VP applicator (A/V = 14.1 m^{-1}), resulting in a greater electrode–soil contact area and a more homogeneous energy distribution within the treated soil volume.

The applicators were subsequently compared for their effects on *Meloidogyne chitwoodi* second-stage juveniles (J2) and *Cyperus esculentus*. Differences between applicator types were observed for both nematode and weed control (Figs. 3 and 4; Table 2). Both applicators reduced *M. chitwoodi* J2 densities

by at least 45%. At 60 Hz, *M. Chitwoodi* reductions reached 91% with the PP applicator (Fig. 3A) and 73% with the VP applicator (Fig. 3B). Applicator performance also varied with field strength. The PP applicator achieved complete suppression of *M. chitwoodi* J2 across the tested frequency range, whereas the VP applicator required approximately twice the field strength to achieve comparable suppression. The greater efficacy of the PP applicator is consistent with the more uniform energy distribution predicted by the electrostatic simulations and the larger electrode–soil interface relative to the treated soil volume.

The effect of applicator type on *C. esculentus* was evaluated across energy densities ranging from 0 to 200 J cm^{-3} and two pulse widths (0.001 and 0.005 s) (Fig. 4A,B). Using the PP applicator, plant biomass declined progressively with increasing energy density, with a stronger response observed at the greater pulse width (0.005 s), indicating greater treatment efficacy (Fig. 4A). In contrast, the VP applicator produced more variable responses across energy densities, with shoot dry weight fluctuating among treatments and greater variability among replicates, as reflected by wider confidence intervals (Fig. 4B). These results are consistent with the heterogeneous electric field distribution produced by the pin geometry, where electrical energy is concentrated near discrete electrode contact points rather than distributed uniformly throughout the treated soil volume. Overall, the PP applicator provided a more uniform and effective delivery of electrical energy, resulting in greater suppression of plant growth compared with the VP configuration.

Because of its higher and more consistent efficacy, subsequent experiments evaluating the effects of PEF on plant-parasitic nematodes, soilborne pathogens, and weeds were conducted using the PP applicator (Table 1).

Table 1
Pulsed electric fields parameters applied for plant-parasitic nematode, soilborne pathogen, and weed propagules suppression.

Species	**Treated pest stage or organ**	**Energy (J cm^{-2})**	**FS (V mm^{-1})**	**FQ (Hz)**	**PD (s)**	**App.**	**N. exp.**
Applicator development							
M. chitwoodi	J2	25	100; 200	0–80	0.005	VP & PP	4
P. neglectus	mix life stages	25	100; 200	0–80	0.005	VP & PP	4
C. esculentus	tuber	0-200	50; 250	100	0.005	VP & PP	4
C. esculentus	tuber	0-200	10; 800	100	0.001; 0.005	VP & PP	4
Weed species effect of field strength							
E. crus-galli	seed	0-200	50, 250	100	0.005	PP	2
D. sanguinalis	seed	0-200	50, 250	100	0.005	PP	2
Nematodes frequency and field strength							
M. chitwoodi	J2	25	200; 400	0-120	0.005	PP	4
P. neglectus	mix life stages	25	200; 400	0-120	0.005	PP	2
Soil pathogens frequency and field strength							
P. cinnamomi	mix life stages	25	100; 200	0–80	0.005	PP	2
P. plurivora	mix life stages	25	100; 200	0–80	0.005	PP	2
V. dahliae	Microsclerotia	25	100; 200	0–80	0.005	PP	2
V. dahliae	Microsclerotia	25	200; 400	0–80	0.005	PP	2

Abbreviations: App – applicator; VP – vertical pin; PP – parallel plate; FS – field strength, FQ – frequency; PD – pulse duration; N. exp. – number of experiments conducted.

Table 2
Summary of analysis of variance for significant factors and interactions for pulsed electric field applications to Meloidogyne chitwoodi and Cyperus esculentus with different applicators.

Meloidogyne chitwoodi			***Cyperus esculentus***		
Frequency (FQ)			*Pulse width (PW)*		
Factors	*Chi sq*	*P*	*Factors*	*Chi sq*	*P*
Frequency	*67.03*	***	*Energy*	*66.24*	***
Applicator	*14.93*	***	*Applicator*	*19.47*	***
FQ	*12.94*	***	*PW*	*5.15*	*
*FQ*Applicator*	*18.26*	**	*Energy * Applicator*	*45.85*	***
*Applicator * FQ*	*9.71*	**	*Applicator * PW*	*2.68*	*0.10*
*P – Probability: 0 '***' 0.001 '**' 0.01 '*' 0.05 '.' 0.1 ' ' 1*					

• Soil Physical and Chemical Changes to PEF treatment

Once we determined that the PP applicator provided more consistent and improved suppression against *M. chitwoodi* and *C. esculentus*, we also monitored the physical responses of the soil in treated pots to increasing energy densities. Soil temperature rose steadily with increasing energy density applied, rising from approximately 35°C at 15 J cm^{-3} to nearly 100°C at 200 J cm^{-3} (Fig. 5A). In addition, at the highest energy density (> 100 J cm^{-3}), soil hardened to form a thermally induced induration, indicating that excessive heat accumulation can alter soil structure (Fig. 5B). In contrast, electrical conductivity remained relatively stable up to 100 J cm^{-3}, with only minor fluctuations, and then increased sharply at the highest dose. Statistical groupings confirmed that temperature differed significantly across energy density, while conductivity showed a marked difference only under the most extreme conditions. These results indicate that although PEF influences both parameters, temperature responds more linearly, whereas conductivity displays a delayed but pronounced increase under high-energy exposure.

The multivariate analysis of soil chemical attributes, based on Mehlich-3 extractions, indicated that PEF application (0, 50, and 200 J cm^{-3}) did not promote statistically significant variations in the multivariate profile (Fig. 5C). PCA explained 50.1% of the total variance in the first two axes (PC1 = 28.2%; PC2 = 21.9%), but no consistent separation among treatments was observed. This was confirmed by ANOVA of the scores (p = 0.496 for PC1; p = 0.622 for PC2) and by PERMANOVA (R^2 = 0.042; p = 0.944). Similarly, redundancy analysis (RDA) showed treatment centroids clustered near the origin and vectors of low magnitude, reinforcing the absence of a detectable effect of energy on soil nutrient availability.

• Effect of PEF on weed propagules

Pulsed electric field treatment using the PP applicator significantly affected shoot biomass of *C. esculentus*, *Digitaria sanguinalis*, and *Echinochloa crus-galli* (Fig. 6). For *C. esculentus* (Fig. 6A), there was a significant effect of energy density ($\chi^2 = 99.62$, $p < 0.001$), field strength ($\chi^2 = 8.83$, $p = 0.002$), and their interaction ($\chi^2 = 26.15$, $p < 0.001$), though the overall downward trend of increasing energy density was more consistent at 50 V mm^{-1} field strength. Shoot biomass remained similar to the nontreated control at energy densities of 25–75 J cm^{-3}, at 50 V mm^{-1}, or 25–150 J cm^{-3} and 250 V mm^{-1}. Biomass declined sharply at ≥ 100 J cm^{-3}, with greater suppression at 50 V mm^{-1} than at 250 V mm^{-1}. Complete biomass elimination occurred at > 125 J cm^{-3} for 50 V mm^{-1} but not at 250 V mm^{-1}. For *D. sanguinalis* (Fig. 6B), energy density significantly affected shoot biomass ($F_{7,45} = 7.36$, $p < 0.001$), field strength ($F_{1,45} = 7.32$, $p = 0.010$), and their interaction ($F_{6,45} = 3.84$, $p = 0.004$). Biomass began to decline at approximately 50 J cm^{-3} at 50 V mm^{-1} field strength and decreased progressively with increasing energy except at 200 J cm^{-3}. Conversely, at 250 V mm^{-1} field strength, biomass reduction began at 75 J cm^{-3} and continued up to 200 J cm^{-3}. For *E. crus-galli* (Fig. 6C), significant effects of energy density ($F_{7,45} = 16.95$, $p < 0.001$), field strength ($F_{1,45} = 8.05$, $p = 0.007$), and their interaction ($F_{6,45} = 3.19$, $p = 0.011$) were observed. Shoot biomass did not decline at 25–100 J cm^{-3} and in some cases exceeded the nontreated control. Substantial reductions in biomass occurred at 150–200 J cm^{-3} for 250 V mm^{-1} and at 200 J cm^{-3} for 50 V mm^{-1}.

• Effect of PEF on plant-parasitic nematodes

PEF markedly reduced plant-parasitic nematode densities compared to the nontreated control (Fig. 7). For *M. chitwoodi* (Fig. 7A), a zero-inflated negative binomial model provided a substantially better fit than a standard negative binomial model (ΔAIC = 11.1) and was therefore retained. *M. chitwoodi* suppression increased markedly with frequency ($p < 0.008$) and field strength ($p < 0.03$). At both field strengths, *M. chitwoodi* density decreased progressively from 30 Hz to 60 Hz, reaching total suppression at 90–120 Hz. For *P. neglectus* (Fig. 7B), density was reduced significantly by field strength ($p < 0.001$), whereas frequency had no significant effect ($p = 0.98$). At 200 V mm^{-1}, nematode reduction ranged from 74% to 93%. Increasing the field strength to 400 V mm^{-1} significantly enhanced efficacy, with suppression levels above 98% at all frequencies.

• Effect of PEF on soilborne pathogens

Overall, field strength and frequency affected the PEF efficacy against all three soilborne pathogens (Figs. 8 and 9). For *P. cinnamomi* (Fig. 8A), there was an effect of frequency ($\chi^2 = 4.04$, $p = 0.044$) and a strong interaction between frequency and field strength ($\chi^2 = 23.24$, $p < 0.001$). *P. cinnamomi* counts were reduced to nondetectable levels at both 100 and 200 V mm^{-1} when applied at the 80 Hz frequency. For *P. plurivora* (Fig. 8B), all treatments reduced pathogen counts compared to the nontreated control. Field strength had a strong effect on *P. plurivora* ppg ($\chi^2 = 15.38$, $p < 0.001$), while pulse frequency alone did not have a significant main effect when averaged across field strength levels ($\chi^2 = 0.88$, $p = 0.35$).

However, we detected a significant field strength × frequency interaction ($\chi^2 = 6.19$, $p = 0.013$), indicating that the effect of field strength (voltage) on propagule count depended on pulse frequency.

Verticillium dahliae response to PEF depended on the pulse frequency ($\chi^2 = 46.97$, $p < 0.001$), whereas field strength alone did not have a significant main effect ($\chi^2 = 0.07$, $p = 0.79$) (Fig. 9). A significant field strength × frequency interaction was also detected ($\chi^2 = 7.52$, $p = 0.006$), demonstrating that the effect of frequency on *V. dahliae* depended on the applied field strength level (voltage). These results indicate that pulse frequency at 80 Hz was the most effective treatment against *V. dahliae*.

Discussion

Pulsed electric field-induced pest suppression is primarily attributed to electroporation [13,14], which occurs when the applied electric field exceeds the critical transmembrane potential of a biological membranes, resulting in reversible or irreversible membrane disruption and loss of cellular homeostasis. Because this mechanism is not species-specific and affects a wide range of biological cells, pulsed electric field (PEF) treatments have been explored as a non-chemical approach for the inactivation of microorganisms, plant tissues, and other biological structures [7,8,15]. In soil systems, this mechanism provides a potential pathway for simultaneously suppressing weeds, nematodes, and soilborne pathogens. Building on earlier work by Riga et al.[6], the present study shows that treatment efficacy is strongly influenced by applicator design and the resulting distribution of electrical energy within the treated soil.

Across experiments, applicator design, energy density, field strength, and pulse frequency interacted to determine treatment outcomes. Among these factors, applicator design emerged as the dominant determinant of efficacy. Increasing energy input resulted in effective suppression only when delivered through the parallel-plate (PP) applicator, whereas the vertical-probe (VP) applicator produced inconsistent responses even at higher energy densities. This outcome likely reflects differences in electric field distribution within the soil volume. Numerical simulations and experimental studies have demonstrated that pulsed electric field chamber geometry strongly influences field uniformity and that the effective electric field strength within a treatment zone often deviates from theoretical estimates derived from electrode spacing. Treatment chambers may also contain transition zones where the electric field is insufficient to induce electroporation yet still contributes to overall energy input and heating [16–18]. Consequently, systems with heterogeneous field distributions may deliver substantial energy without achieving the threshold electric field required for biological inactivation. The strong suppression observed with the PP applicator therefore likely reflects more uniform field delivery and greater soil volume exposed to effective electric field intensities.

Pulse frequency significantly enhanced nematode suppression, with higher frequencies resulting in greater mortality. Field strength also contributed to suppression, although its effect was more modest and consistent across treatments, particularly under the PP configuration. Previous studies have similarly identified electric field strength as a key parameter governing PEF treatment efficiency, with

microbial and cellular inactivation occurring only when the applied field exceeds the electroporation threshold[12,19]. Interaction analyses in the present study confirmed that increases in energy input and field strength translated into improved biological control, particularly when combined with uniform electric field delivery, highlighting the integrated nature of PEF process parameters.

Weed responses to PEF were species dependent. *D. sanguinalis* was highly susceptible, exhibiting near-complete biomass suppression at intermediate to high energy densities regardless of field strength. *Cyperus esculentus* showed moderate sensitivity; biomass reductions became pronounced at higher energy inputs, particularly under elevated field strength. In contrast, *E. crus-galli* was the species most tolerant to PEF; it maintained biomass at low to moderate energy densities and responded primarily to the highest doses. Previous studies have shown that pulsed electric field exposure can produce contrasting responses in plant tissues depending on treatment intensity and duration. At relatively low electric field strengths, PEF has been reported to stimulate seed germination and early seedling growth in several crop species, including lettuce, wheat, tomato, chickpea, and barley [20]. These stimulatory effects have been associated with enhanced membrane permeability, increased enzymatic activity, and improved metabolic processes in germinating seeds. In contrast, higher electric field strengths or longer pulse durations often lead to germination inhibition or cellular damage due to irreversible electroporation and disruption of membrane integrity. For example, lettuce seedlings exhibited growth stimulation at 20–100 V mm^{-1} but inhibition at higher intensities, while *Arabidopsis thaliana* L. and *Triticum aestivum* L. showed similar intensity-dependent responses [20]. No previous report of the effect of PEF on *C. esculentus* tubers was identified. Previous work on *C. esculentus* seeds exposed to repetitive pulsed electric fields reported reduced germination when peak voltages of 6–15 kV were applied across electrode gaps of 4–10 mm, corresponding to estimated field strengths of approximately 600–3750 V mm^{-1} [21]. The reported field strengths in that study are substantially higher than those applied in the present study (50–400 V mm^{-1}), suggesting that effective suppression of underground propagules may depend not only on peak field strength but also on pulse duration, cumulative energy delivery, and the electrical conduction properties of the surrounding soil matrix. Such interspecific variability is consistent with electroporation theory, which predicts that the induced transmembrane potential depends on cellular dimensions and electrical properties[22]. Larger cells experience greater induced membrane potentials at a given external field strength and therefore may reach electroporation thresholds more readily[23]. However, species-level responses in intact plant tissues are also influenced by cell wall structure, tissue organization, membrane composition, and water content, all of which can modify the distribution of the electric field and electroporation thresholds. Taken together, these results indicate that seed or plant propagule responses to PEF depend on field strength and the total energy delivered, and that high energy (> 100 J cm^{-3}) is required to reliably eliminate plant propagules.

For plant-parasitic nematodes and soilborne pathogens, field strength (25 J cm^{-3}) was the parameter most influential on survival and viability. Similar relationships have been reported for microbial inactivation by PEF, where field strength governs the magnitude of induced membrane potentials and determines whether reversible or irreversible electroporation occurs[6,7,19]. Pulse frequency further

enhanced suppression of *M. chitwoodi*, whereas responses of *P. neglectus* were less consistent, with partial survival observed at lower field strengths. These differences likely reflect variation in morphological and biophysical characteristics among organisms.

Pulsed electric field treatments strongly suppressed *Phytophthora* spp. and *V. dahliae*, with near-complete inactivation observed at higher field strength and frequency combinations (Fig. 8–9). The strong suppression of all three species in the present study is consistent with recent work demonstrating that pulsed electric fields effectively inactivate soilborne fungal pathogens. For example, Chen et al. [24]investigated PEF sterilization of *Fusarium oxysporum* in greenhouse soils and reported that fungal mortality increased rapidly with electric field strength, reaching approximately 90–99% lethality when electric field strength increased from 5 to 14 kV cm^{-1}.[24] *V. dahliae* forms microsclerotia and *Phytophthora* species form oospores or chlamydospores that can survive in soil for extended periods and are difficult to control with conventional management practices[25]; the strong response observed here suggests that PEF could be a promising non-chemical soil disinfestation strategy for both plant pathogenic genera.

Increasing applied energy elevated soil temperature and electrical conductivity, reflecting enhanced electrothermal excitation and increased ionic mobility during treatment. Moderate temperature increases may contribute synergistically to membrane destabilization and biological damage, as mild heating is known to enhance the effectiveness of PEF treatments in biological systems. Despite these physical changes, soil chemical properties remained largely unaffected across treatments, indicating that PEF application up to 200 J cm^{-3} did not substantially alter bulk nutrient availability or soil chemistry. Nonetheless, PEF is known to alter soil physicochemical properties when treatment durations are prolonged (days), leading to ion electromigration, diffusion, and altered soil pH[3]. The short treatment duration we implemented here focused on a rapid biological suppression of pests and may not have altered chemical properties to a detectable level. Furthermore, effective suppression of plant-parasitic nematodes and soilborne pathogens was achieved at substantially lower energy inputs, 25 J cm^{-3}, suggesting that biological control may be achievable with short durations and lower energy levels. Although very high energy densities may induce localized heating or structural changes in soil structure, such conditions are unlikely to be economically viable as a soil disinfestation strategy in commercial agricultural systems.

Overall, PEF treatment effectively suppressed plant-parasitic nematodes, soilborne pathogens, and weed propagules in soil, with treatment efficacy determined by applicator design and electrical parameters. Uniform electric field delivery was essential for consistent biological suppression, and optimal control depended on appropriate combinations of energy density, field strength, and pulse frequency. Responses varied among target organisms, emphasizing the importance of species-specific optimization of PEF parameters. In the present study, suppression of nematodes and soilborne pathogens was generally more consistent and demanded less energy than suppression of weed propagules, suggesting that soil-applied PEF may be particularly well suited for the management of microorganisms. In contrast,

effective weed control with PEF likely requires direct exposure of aboveground tissues[26,27]. Future research should therefore focus on optimizing PEF strategies for weed management, including alternative exposure pathways such as foliar or plant-targeted electrical delivery systems that may improve energy transfer to plant tissues. While PEF induced strong biological effects, impacts on bulk soil chemistry were minimal under the conditions tested. Together, these findings support the potential of PEF as a non-chemical soil disinfestation technology and highlight the need for further research to refine applicator design and evaluate performance under field conditions.

Methods

• Plant-parasitic nematode inoculum preparation

Meloidogyne chitwoodi inoculum, originally collected from a potato field in Hermiston, OR, was reared on tomato (*Solanum lycopersicon* 'Rutgers') in a greenhouse. The tomato plants were harvested, and egg masses on roots were hand-picked into a scintillation vial containing water[28]. A 0.05% sodium chloride solution was then added to the vial and shaken for 3 min. The egg solution was poured over nested 250- and 25-µm sieves, rinsed with water, and the eggs retained on the 25-mm sieve. The collected eggs were either retained for experiments or were placed in a hatching chamber[28] to obtain second-stage juveniles (J2) after 5 to 7 days. *M. chitwoodi* J2 were collected daily and held at 4°C until used in experiments. *Pratylenchus neglectus* inoculum was originally collected from a wheat field in Pendleton, OR, and maintained on wheat (*Triticum aestivum* 'Scarlett') in a greenhouse. To obtain *P. neglectus* for experiments, plants were destructively harvested, roots washed free of soil, and then placed under intermittent mist (15-sec mist every 2 min) for five days[29]. The collected nematodes were held at 4°C until use. Solutions containing plant-parasitic nematodes were adjusted to achieve desired inoculation densities.

• Soilborne pathogen inoculum preparation

Phytophthora cinnamomi (isolate R056) and *P. plurivora* (isolate R003) inocula were prepared using previously published methods[30]. Isolates were cultured on 20 mL of clarified V8 juice agar (composed of 3.4 g $CaCO_3$ mixed with 340 mL of filtered V8 juice, diluted 1:4 with distilled water, and supplemented with 17 g of agar L^{-1}) for seven days. The colonized agar was then cut into 1.5 cm² pieces and added to a spawn bag (Fungi Perfecti, Olympia, WA) containing 2 L of clarified V8 juice broth (made from 150 mL of clarified V8 juice, $CaCO_3$, and 1,850 mL of distilled water) mixed with 3 L of dry coarse vermiculite that had been autoclaved three times at 48-hour intervals. Spawn bags were incubated in the dark at 20°C for six weeks, with weekly mixing for aeration. Inoculum density was assessed by dilution plating onto PARP (pimaricin, ampicillin, rifampicin, pentanitrochlorobenzene), a semi-selective medium for pythiaceous species[31], and then stored at 20°C until used within 1 week in experiments.

Verticillium dahliae inoculum was produced using a modified method from López-Escudero et al.[32]. A mixture of four isolates from raspberry were[6] cultured on plates containing 20 mL of potato dextrose

agar for six days at 24°C. Conidia were washed from the surface with sterile distilled water, and 0.5 ml of the suspension was plated onto PDA covered with a sterilized disk of cellophane (Ultra Clear Cellophane, Research Products International, Mount Prospect, IL) and incubated for 14 days at 22°C. Microsclerotia were harvested from the plates and mixed with sterilized sand, then air-dried for 48 hours at 28°C. Inoculum density was estimated using an Andersen sampler[33] to distribute 0.05 g of infested sand on ten plates of NP10[34] a semi-selective medium for *V. dahliae*. Inoculum was stored at 20°C until used within 1 week in experiments.

• Weed propagule inoculum preparation

Seeds of *D. sanguinalis*, *E. crus-galli*, and tubers of *C. esculentus* were manually cleaned to remove any foreign material and stored at room temperature in paper bags until used. Before use in experiments, seeds and tubers were placed in 5°C water for 12 h.

• PEF Delivery System

Pulsed electric field (PEF) treatments were delivered using a pulsed Direct Energy System (DES; Lisi Global Inc., Richland, WA, USA). The system generates capacitive-decay pulses that are discharged through electrodes inserted into the soil. We evaluated two electrode configurations: vertical pins (VP) and parallel metallic plates (PP) (Fig. 1A, B). Each configuration produces distinct electric field distributions while maintaining predetermined electric field gradients (V mm^{-1}). All treatments were applied to sterilized soil placed in square plastic containers with a top width of 8.9 cm, a bottom width of 6.4 cm, and a depth of 8.9 cm. Containers were filled with approximately 500 cm^3 (5×10^{-4} m^3).

The VP applicator was a prototype designed for soil applications (Direct Energy System, Lisi Global Inc., Richland, WA, USA; Fig. 1A). The device consisted of two rows of four metallic pins separated by 0.07414 m, with polarity assigned by row (one positive row and one negative row). Each pin was 0.00635 m in diameter and inserted to a depth of 0.0988 m. Within each row, pins were spaced at 0.0254 m, resulting in a treated swath of 0.0762 m. The treated soil volume, defined as the footprint between the outermost pins multiplied by insertion depth, was $5.58 \times 10^{-4} m^3$. Considering only the inward-facing half of the lateral pin surface as the active electrode interface (total electrode surface area = 7.88×10^{-3} m^2), the electrode surface area to treated soil volume ratio (A/V) was 14.1 m^{-1}.

The PP applicator consisted of two aluminum plates (0.0508 × 0.0508 m; thickness 0.0031 m) separated by 0.0741 m. The treated soil volume, defined as the interelectrode volume between the opposing plate faces, was 1.91×10^{-4} m^3. Considering only the inward-facing surface of each plate as the active electrode interface (total electrode surface area = 5.16×10^{-3} m^2), the electrode surface area to treated soil volume ratio (A/V) was 27.0 m^{-1}, representing an electrode–soil interface 1.91 times larger than that of the VP applicator.

We estimated the spatial distribution of electric potential and resulting electric field between electrodes using a numerical electrostatic model assuming a homogeneous and perfectly uniform medium. Under these conditions, the electric potential (ϕ) satisfies Laplace's equation ($\nabla^2\phi = 0$), which describes the

steady-state distribution of potential in the absence of internal charge sources. We calculated the electric field (E) from the potential gradient according to $E = -\nabla\phi$, and the field magnitude was determined as $|E| = \sqrt{[(\partial\phi/\partial x)^2 + (\partial\phi/\partial y)^2]}$. The equations were solved on a two-dimensional grid using an iterative relaxation scheme based on weighted Jacobi/successive over-relaxation methods, with electrode regions treated as fixed-potential (Dirichlet) boundaries.

For the PP configuration, electrodes were modeled as two parallel boundaries separated by 5 cm. Boundary conditions were defined such that $\phi(0,y) = +V/2$ and $\phi(W,y) = -V/2$, where W represents the electrode spacing. Under these conditions, the analytical solution is linear, producing a uniform electric field between the plates given by $|E| = V/W$. Target electric field gradients were imposed by adjusting the applied voltage difference (ΔV) according to $\Delta V = (V\ mm^{-1}) \times 50\ mm$, with electrode potentials assigned as $\pm \Delta V/2$.

Electrodes of the pin electrode configuration were represented as circular Dirichlet regions embedded within the computational grid, corresponding to cylindrical electrodes arranged in two opposing columns. Solving Laplace's equation numerically with these embedded boundary conditions provided the electric potential distribution. Because Laplace's equation is linear, the normalized potential field was scaled to the desired applied voltage difference according to $\phi\_scaled = \phi\_norm \times (\Delta V/2)$. Electric field components were estimated using central finite-difference approximations of the potential gradients, where $Ex \approx -(\phi_{i+1,} - \phi_{i-1,})/(2\Delta x)$ and $Ey \approx -(\phi_{i,+1} - \phi_{i,-1})/(2\Delta y)$. The resulting electric field magnitude was expressed as $V\ mm^{-1}$ and visualized spatial variations in field intensity across the treatment domain.

Energy density was defined as the total electrical energy delivered normalized to the treated soil volume ($J\ cm^{-3}$). Total energy input was calculated as the product of the energy delivered per pulse ($J\ pulse^{-1}$) and the number of pulses applied, divided by the treated soil volume. The energy delivered per pulse (E_pulse) was calculated from the instantaneous voltage and current waveforms according to: $E\_pulse = \int V(t)\ I(t)\ dt$, where V(t) is the voltage (V) and I(t) is the current (A) as a function of time during a single pulse. All treatments consisted of a single, uninterrupted pulse train with identical pulse waveform and energy across all pulses. Differences in energy density among treatments were due to the variance in the number of pulses delivered. Soil electrical conductivity was analyzed prior to each experiment and treatment duration adjusted accordingly, to ensure consistent energy delivery across replicates. Applied energy densities ranged from $2.5 \times 10^7\ J\ cm^{-3}$ for nematodes and soilborne pathogens to $2.0 \times 10^8\ J\ cm^{-3}$ for weed seeds and tubers (Table 1).

• PEF experimental design and evaluations

A uniform pasteurized dry soil mix (1:1 sand to loam) was used to ensure consistency in experiments with the soil pests. The experimental unit consisted of a 10 x 10 cm plastic pot containing approximately 500 cc of soil. Treatments were replicated four times, and each experiment was conducted twice.

The VP and PP applicators were evaluated for energy delivered to weed seeds at variable energy densities and field strengths (Table 1). The frequency and pulse rate remained constant at 100 Hz and 0.005 pulses per second, respectively. Twenty seeds of *D. sanguinalis* and *E. crus-galli* were separately planted in soil-mix-filled pots at a depth of approximately 1 cm. Six tubers of *C. esculentus* were similarly planted at a depth of approximately 1 cm. The pots were moved to the greenhouse after treatment, and weeds were allowed to grow for eight weeks. The aboveground portion of the plant was harvested, and the roots rinsed free of soil under running tap water. All plant material was placed in a 70 ºC oven for three days, and then weighed to determine the dry weight of the entire plant.

See Table 1 for our evaluation of the effect of the VP and PP applicators on plant-parasitic nematodes, with energy applied at the noted field strengths and frequencies. The total energy delivered and pulse were held constant at J cm^{-3} of soil and 0.005 pulses sec^{-1}, respectively. Pots were filled with the soil mix, and 1,000 *M. chitwoodi* J2 or mixed stages of *P. neglectus* were added to three 2 cm deep holes in each pot in approximately 5 mL water. Energy was applied following the specific profile for each nematode (Table 1). After treatment, the soil in the pots was placed into resealable plastic bags, thoroughly mixed, and then moved to the laboratory for analysis. To evaluate the efficacy of PEF on *M. chitwoodi* and *P. neglectus*, 50 g of the soil was placed on a Baermann funnel for 5 days[35]. Plant-parasitic nematodes collected from funnels were counted using an inverted microscope.

Only the PP applicator was used in experiments with soilborne pathogens; energy was delivered at the field strengths and frequencies listed in Table 1. The total energy and pulse delivered remained constant at 25 J cm^{-3} of soil and 0.005 pulses sec^{-1}, respectively. *Verticillium* and *Phytophthora* pathogen inocula were mixed separately into the dry soil mix to achieve a final concentration of ≥ 75 propagules per gram of soil (ppg). Infested soil was then distributed into pots for treatment. After treatment, efficacy was evaluated by dilution plating (for *Phytophthora* species) or using an Andersen sampler (for *V. dahliae*), as described above.

We also evaluated the effect of the PP applicator on soil physical and chemical. Soil, adjusted to a previously determined optimal moisture content for electrical conductivity, was placed in containers. Energy densities from 1 to 200 J cm^{-3} were applied, and temperature (°C) and electrical conductivity (S m^{-1}) were recorded immediately after each application. A K-type thermocouple probe was used to simultaneously assess heat generation and ionic mobility. For chemical characterization, soil samples were analyzed using the Mehlich-3 extraction method, which enables the simultaneous determination of macro- and micronutrients, by a certified commercial laboratory following standardized protocols for sample preparation, extraction, and quantification. The resulting dataset included concentrations of Ca, Mg, K, P, Fe, Mn, Zn, and Cu, expressed in mg kg^{-1} of soil.

• Data analysis

All analyses were performed using R software (version 4.5.3; R Core Team, Vienna, Austria). Data were analyzed using general linear models (GLM) for each target organism. To meet the assumptions of normality and homoscedasticity, the data were square root transformed. Field strength and frequency

were included as fixed effects, with frequency nested within field strength. Post-hoc comparisons between treatment were performed using Tukey's Honest Significant Difference (HSD) test at a 5% significance level, allowing the identification of statistically distinct treatment groups.

Weed seed data were analyzed using ANOVA. Means were separated using Tukey's honest significant difference test ($p \leq 0.05$). To assess the association between field strengths and frequencies, a correlation analysis was performed. Random-effects structures were simplified when variance components were estimated as zero, retaining only supported random effects.

Soil chemical data (Mehlich-3) were analyzed by principal component analysis (PCA) using the prcomp() function after centering and scaling. Differences among energy densities (0, 50, and 200 J cm^{-3}) were assessed by ANOVA with Tukey's test ($p < 0.05$). A permutational multivariate analysis of variance (PERMANOVA, 999 permutations, Euclidean distance) and redundancy analysis (RDA) were also performed.

Declarations

Competing Interests

The author Jason Crisp is the Chief Executive Officer of Lisi Global Inc., which develops pulsed electric field technology used in this study. The remaining authors declare no competing interests.

Funding:

This work was funded, in part, by the USDA-NIFA Methyl Bromide Transitions Program 2022-51102-38259, the Horticulture Research Institute, the Oregon Association of Nurseries, and USDA-ARS project 2072-22000-046-000-D. Mention of trade names or commercial products in this publication is solely for the purpose of providing specific information and does not imply recommendation or endorsement by the U.S. Department of Agriculture. USDA is an equal opportunity provider and employer.

Author Contribution

T.B. – field methodology, data curation, field methodology, formal analysis, writing-original draft, writing-review & editing; P.M.S – field methodology, field methodology, reviewing & editing; M.L.M. – funding acquisition, conceptualization, field methodology, project administration, supervision, writing-review & editing; J.E.W. – funding acquisition, conceptualization, field methodology, project administration, supervision, writing-review & editing; J.C - funding acquisition, conceptualization, field methodology; I.Z. – funding acquisition, conceptualization, field methodology, project administration, supervision, writing-review & editing

Acknowledgments

The authors thank JF Schmidth Nursery, and Robinson Nursery for assisting in the studies. To Kim Graham and Bryan Beck for technical assistance in preparing and quantifying pathogen inoculum.

Data Availability

The data that support the findings of this study are available from the corresponding author upon reasonable request.

References

1. Gullino, M. L., Garibaldi, A., Gamliel, A. & Katan, J. Soil disinfestation: from soil treatment to soil and plant health. *Plant. Dis.* **106**, 1541–1554. 10.1094/PDIS-09-21-2023-FE (2022).
2. Mirabella, A., Ciriello, M., Rouphael, Y., El-Nakhel, C. & Altucci, C. Sustainable soil disinfestation approaches in crop production: from chemical dependency to ecological resilience. *Horticulturae* **12**, 189, doi:ARTN 189.
3. 3 Abou-Shady, A. & 3390/horticulturae12020189 et al. A comprehensive analysis of the advantages and disadvantages of pulsed electric fields during soil electrokinetic remediation. *Int. J. Environ. Sci. Technol. (Tehran)* 22, 3895–3925 (2025). 4 Ghoshal, G. Comprehensive review on pulsed electric field in food preservation: Gaps in current studies for potential future research. *Heliyon* 9, e17532, (2026). https://doi.org/10.1016/j.heliyon.2023.e17532 (2023). 5 Jeyamkondan, S., Jayas, D. & Holley, R. Pulsed electric field processing of foods: a review. *J. Food Prot.* 62, 1088–1096, doi:https://doi.org/10.4315/0362-028x-62.9.1088 (1999). 6 Riga, E., Crisp, J. D., McComb, G. J., Weiland, J. E. & Zasada, I. A. Directed energy system technology for the control of soilborne fungal pathogens and plant-parasitic nematodes. *Pest Manage. Sci.* 76, 2072–2078, doi:https://doi.org/10.1002/ps.5745 (2020). 7 Grahl, T. & Märkl, H. Killing of microorganisms by pulsed electric fields. *Applied Microbiology and Biotechnology* 45, 148–157, doi:https://doi.org/10.1007/s002530050663 (1996). 8 Sale, A. & Hamilton, W. Effects of high electric fields on micro-organisms: III. Lysis of erythrocytes and protoplasts. *Biochimica et Biophysica Acta (BBA)-Biomembranes* 163, 37–43, doi:https://doi.org/10.1016/0005-2736(68)90030-8 (1968). 9 Miranda, J., Membrillo-Hernandez, J., Tabche, M. & Soberón, M. *Rhizobium* etli cytochrome mutants with derepressed expression of cytochrome terminal oxidases and enhanced symbiotic nitrogen accumulation. *Applied Microbiology and Biotechnology* 45, 182–188, doi:https://doi.org/10.1007/s002530050668 (1996). 10 Kim, W.-S. et al. In situ field scale electrokinetic remediation of multi-metals contaminated paddy soil: Influence of electrode configuration. *Electrochimica Acta* 86, 89–95, doi:10.1016/j.electacta.2012.02.078 (2012).
4. Kim, J. H., Ham, G. H., Kim, S. J. & Choe, Y. S. Improvement in uniformity of co-linear pulsed electric field treatment chamber by sub-electrodes and its optimization. *J. Food Process. Eng.* **47**, e14727

(2024).

5. Pataro, G., Senatore, B., Donsì, G. & Ferrari, G. Effect of electric and flow parameters on PEF treatment efficiency. *J. Food Eng.* **105**, 79–88. https://doi.org/10.1016/j.jfoodeng.2011.02.007 (2011).
6. Saulis, G. Electroporation of cell membranes: the fundamental effects of pulsed electric fields in food processing. *Food Eng. Rev.* **2**, 52–73. 10.1007/s12393-010-9023-3 (2010).
7. Sun, S. et al. High voltage pulsed electric field: A novel method for killing parasitic eggs on the surface of raisins. *Food Res. Int.* **196**, 115127. 10.1016/j.foodres.2024.115127 (2024).
8. Arshad, R. N. et al. Pulsed electric field: A potential alternative towards a sustainable food processing. *Trends Food Sci. Technol.* **111**, 43–54. https://doi.org/10.1016/j.tifs.2021.02.041 (2021).
9. Buckow, R., Baumann, P., Schroeder, S. & Knoerzer, K. Effect of dimensions and geometry of co-field and co-linear pulsed electric field treatment chambers on electric field strength and energy utilisation. *J. Food Eng.* **105**, 545–556. 10.1016/j.jfoodeng.2011.03.019 (2011).
10. Schottroff, F. et al. Development of a continuous pulsed electric field (PEF) vortex-flow chamber for improved treatment homogeneity based on hydrodynamic optimization. *Front. Bioeng. Biotechnol.* **8**, 340. 10.3389/fbioe.2020.00340 (2020).
11. Van den Bosch, H. Chamber design and process conditions for pulsed electric field treatment of food. *Food preservation pulsed Electr. fields*, 70–93 (2007).
12. Alvarez, I., Pagan, R., Condon, S. & Raso, J. The influence of process parameters for the inactivation of *Listeria monocytogenes* by pulsed electric fields. *Int. J. Food Microbiol.* **87**, 87–95. https://doi.org/10.1016/s0168-1605(03)00056-4 (2003).
13. Attri, P. et al. Outcomes of pulsed electric fields and nonthermal plasma treatments on seed germination and protein functions. *Agronomy* **12**, 482doiARTN482
14. 21 Bokka, 3390/agronomy12020482, Li, R., Foshee, S. & Kirkici, H. W.in *2009 IEEE Pulsed Power Conference.* 962–964 (IEEE). 22 Ben Ammar, J., Lanoiselle, J. L., Lebovka, N. I., Van Hecke, E. & Vorobiev, E. Impact of a pulsed electric field on damage of plant tissues: effects of cell size and tissue electrical conductivity. *J. Food Sci.* 76, E90-E97, (2022). 10.1111/j.1750-3841.2010.01893.x (2011). 23 Schwan, H. in *Electroporation and electrofusion in cell biology* 3–21 (Springer, 1989). 24 Chen, J. et al. Effects of pulsed electric fields on the elimination of *Fusarium oxysporum* in greenhouse soil. *Agriculture* 14, 2158, doi:ARTN 2158.
15. 25 3390/agriculture14122158 et al. Late-summer disease symptoms in western washington red raspberry fields associated with co-occurrence of *Phytophthora rubi*, *Verticillium dahliae*, and *Pratylenchus penetrans*, but not Raspberry bushy dwarf virus. *Plant Dis* 102, 938–947, (2024). 10.1094

    Bloomer, D. J., Harrington, K. C., Ghanizadeh, H. & James, T. K. The electric spatula: Killing weeds with pulsed microshocks from a flat-plate electrode. *Agronomy* 13, 2694, doi:https://doi.org/10.3390/agronomy13112694 (2023). 28 Zasada, I. A., Riga, E., Pinkerton, J. N.,

Wilson, J. H. & Schreiner, R. P. Plant-parasitic nematodes associated with grapevines, *Vitis vinifera*, in Washington and Idaho. *Am. J. Enol. Vitic.* 63, 522–528, doi:https://doi.org/10.5344/ajev.2012.12062 (2012). 29 Zasada, I. A., Weiland, J. E., Han, Z., Walters, T. W. & Moore, P. Impact of *Pratylenchus penetrans* on establishment of red raspberry. *Plant Dis* 99, 939–946, doi:https://doi.org/10.1094/PDIS-09-14-0980-RE (2015). 30 Weiland, J. E., Scagel, C. F., Grünwald, N. J., Davis, E. A. & Beck, B. R. *Phytophthora* species differ in response to phosphorous acid and mefenoxam for the management of *Phytophthora* root rot in rhododendron. *Plant Dis* 105, 1505–1514, doi:https://doi.org/10.1094/PDIS-09-20-1960-RE (2021). 31 Kannwischer, M. & Mitchell, D. The influence of a fungicide on the epidemiology of black shank of tobacco. *Phytopathology* 68, 1760–1765, doi:https://doi.org/10.1094/Phyto-68-1760 (1978). 32 López-Escudero, F., Mwanza, C. & Blanco-López, M. Reduction of *Verticillium dahliae* microsclerotia viability in soil by dried plant residues. *Crop Prot* 26, 127–133, doi:https://doi.org/10.1016/j.cropro.2006.04.011 (2007). 33 Butterfield, E. & DeVay, J. Reassessment of soil assays for *Verticillium dahliae*. *Phytopathology* 67, 1073–1078, doi:https://doi.org/10.1094/Phyto-67-1073 (1977). 34 Kabir, Z., Bhat, R. & Subbarao, K. V. Comparison of media for recovery of *Verticillium dahliae* from soil. *Plant Dis* 88, 49–55, doi:https://doi.org/10.1094/PDIS.2004.88.1.49 (2004). 35 Baermann, G. Eine einfache methode zur auffindung von Ancylostomum (Nematoden) larven in erdproben. *Geneeskd Tijdschr Ned Indie* 57, 131–137 (1917).

Figures

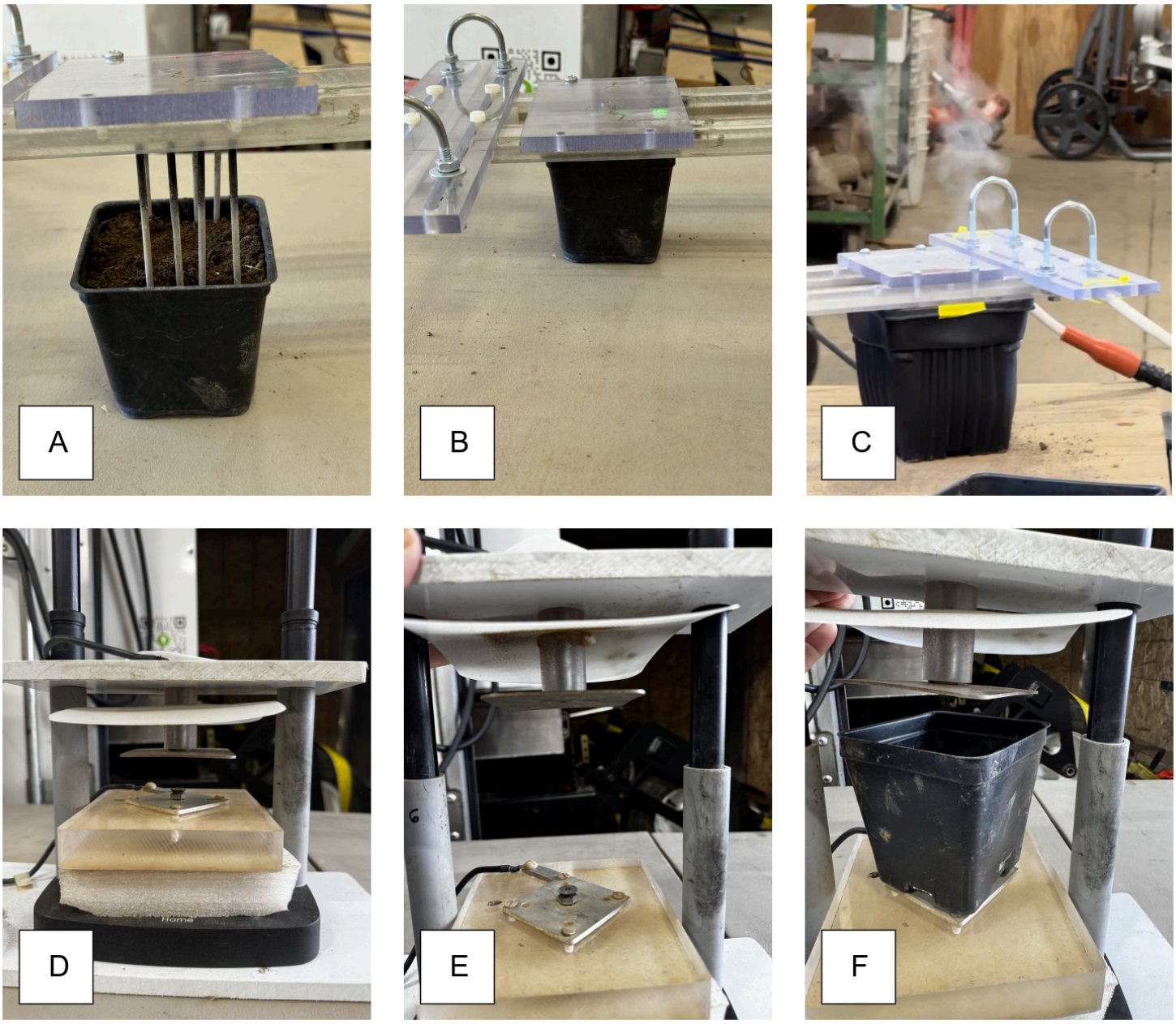

Figure 1

The Pulsed Electrical Field (PEF) application system used to treat weeds, plant-parasitic nematodes and soilborne pathogens in pots containing soil. The vertical pins applicator consisted of eight metal electrode (0.32 cm diameter and 7.62 cm in length) organized in two rows of four spaced at 15 cm apart between rows and 1.27 cm apart within row (A). The vertical pins were completely inserted into the soil for treatment (B). The amount of energy applied was controlled by the number of pulses, field strength, and pulse frequency (C). A commercially available can crusher frame was repurposed as the structural base for the parallel plate applicator (D). The spring crushing mechanism was reversed, and the rigid vertical frame was adapted to securely mount the electrode assembly on the top and bottom of the apparatus (E). The springs pressed the plates downward ensuring proper electrode and soil contact during operation (F).

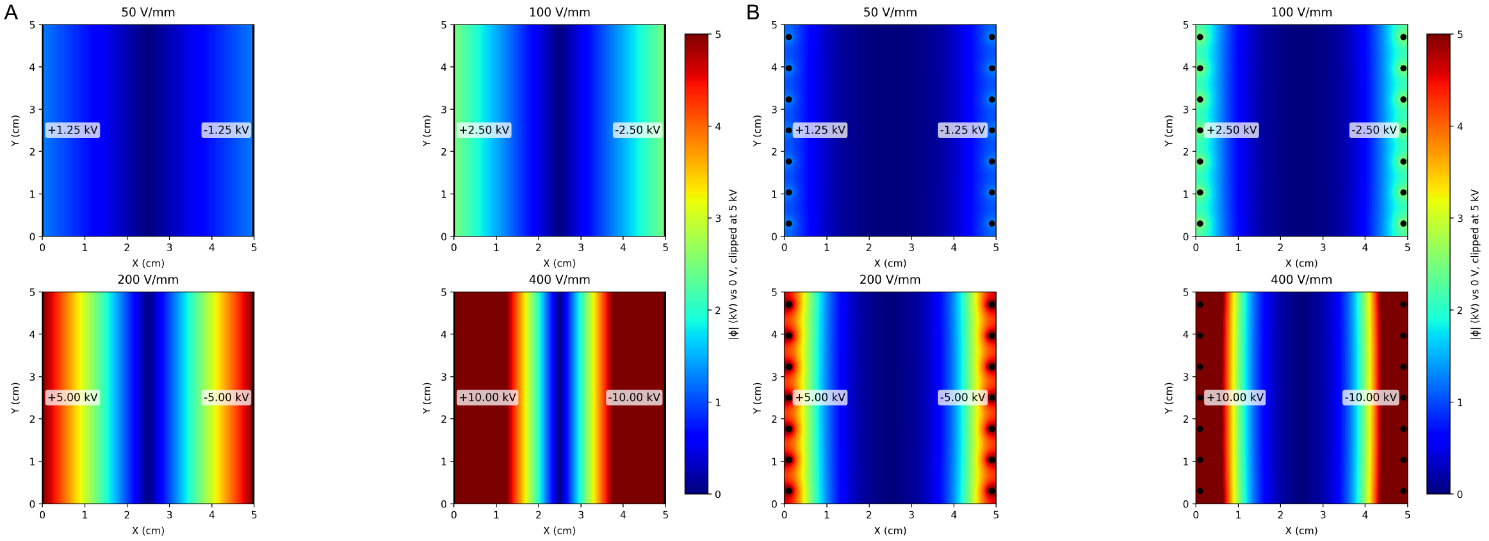

Figure 2

Plan view of the simulated electric potential distribution between two electrodes separated by 5 cm for two electrode configurations. (A) Parallel plates and (B) and vertical pin electrode geometry. Simulations were performed at electric field gradients of 50, 100, 200, and 400 V mm⁻¹. Color scale represents electric potential magnitude |Φ| (kV), capped at ±10 kV. The PP plate electrodes produce a more uniform electric field across the domain, whereas, VP electrodes generate highly localized potential gradients near the electrode surface.

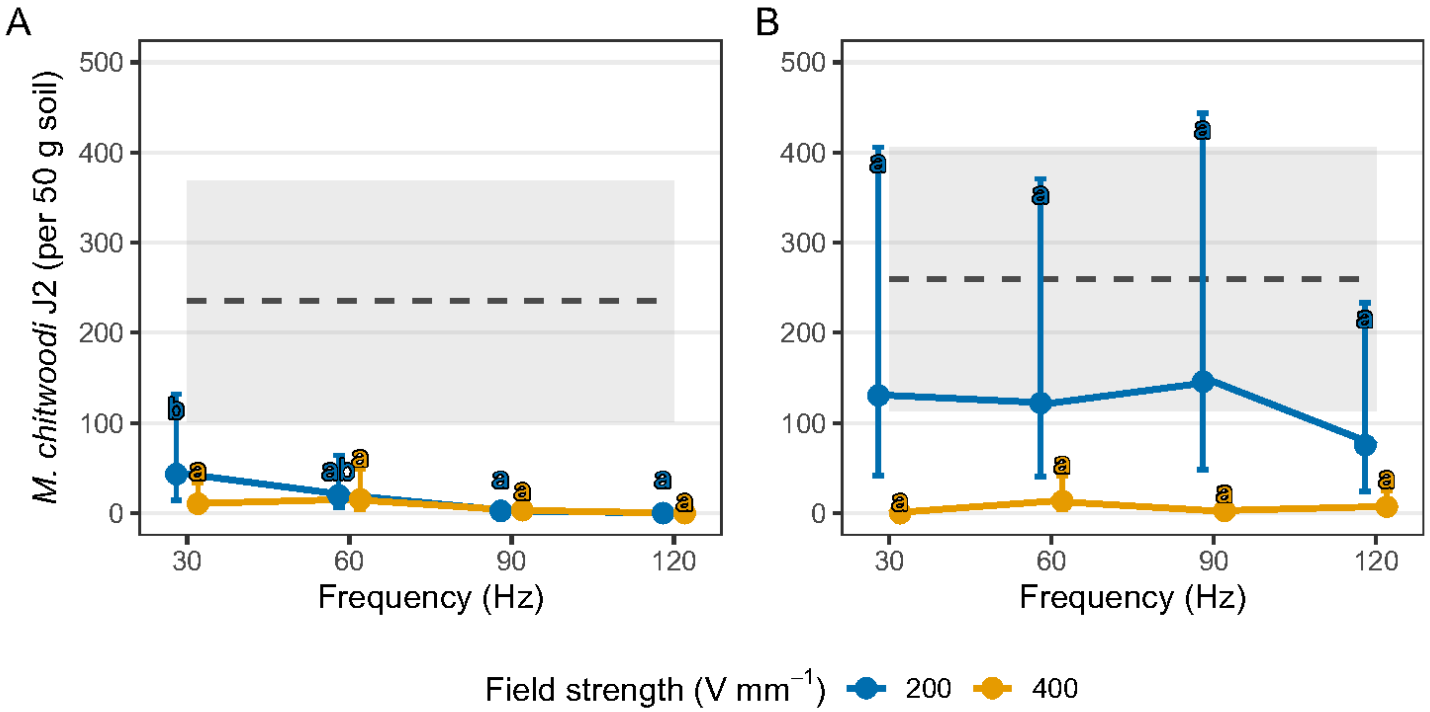

Figure 3

Meloidogyne chitwoodi second-stage juvenile (J2) response to 25 J cm^{-3} energy density applied at 200 and 400 V mm^{-1} field strengths using the parallel plate (A) or the vertical pin (B) applicators. Means followed by different letters within applicator type and frequency are statistically different according to Sidak's test. Means and standard error of means (n = 8) are pooled from two studies. The dashed line and shaded area represent the mean and 95% confidence interval of the nontreated control.

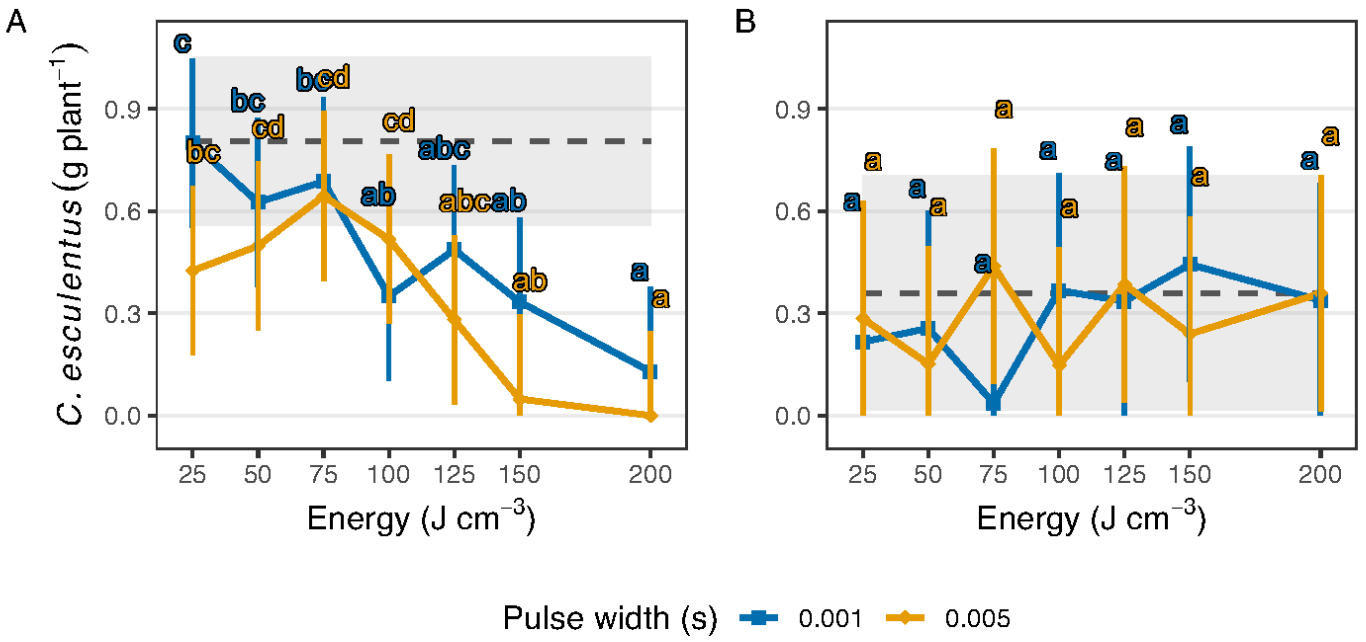

Figure 4

Cyperus esculentus tuber response to energy densities applied from 25 to 200 J cm^{-3} at pulse durations of 0.001 or 0.005 s with the parallel plate (A) or the vertical pin (B) applicators. Means followed by different letters within applicator type and pulse width are statistically different according to Sidak's test. Means and standard error of means (n = 8) are pooled from two studies. The dashed line and shaded area represent the mean and 95% confidence interval of the nontreated control.

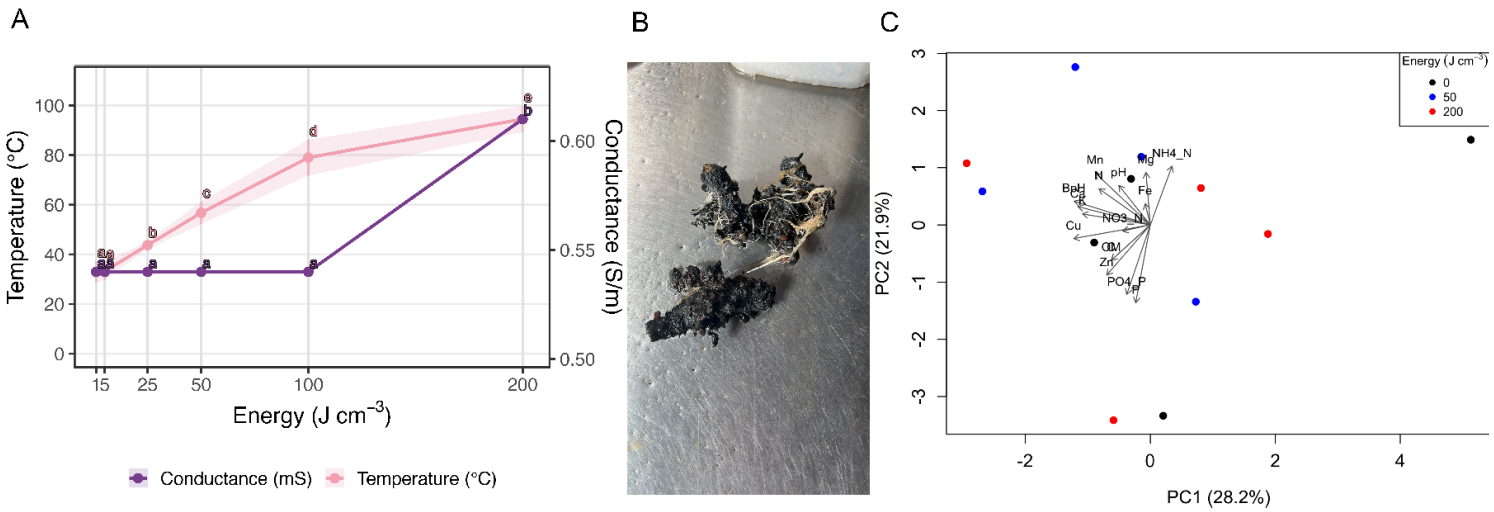

Figure 5

(A) Soil temperature (°C) and electrical conductivity (S m⁻¹) after the application of pulsed electrical field (PEF) at 200 and 400 V mm^{-1} using the parallel plate applicator. Data represent means± standard error (n = 8). Different letters indicate significant differences among energy densities according to Tukey's HSD test ($p < 0.05$). (B) Thermally induced induration of soil observed after PEF treatment at the highest energy input (200 J cm-3). The darkened and compacted soil aggregates, with visible root remnants embedded in the matrix, illustrate the localized overheating effect occurring at the soil–electrode interface. (C) Principal component analysis (PCA) of soil chemical attributes (Mehlich-3) after the application of PEF to deliver energy densities of 0, 50, and 200 J cm⁻³. The first two components explained 50.1% of the total variance (PC1 = 28.2%; PC2 = 21.9%). Symbols represent individual samples and colors indicate energy treatments. No significant separation among treatments was detected ($p > 0.05$).

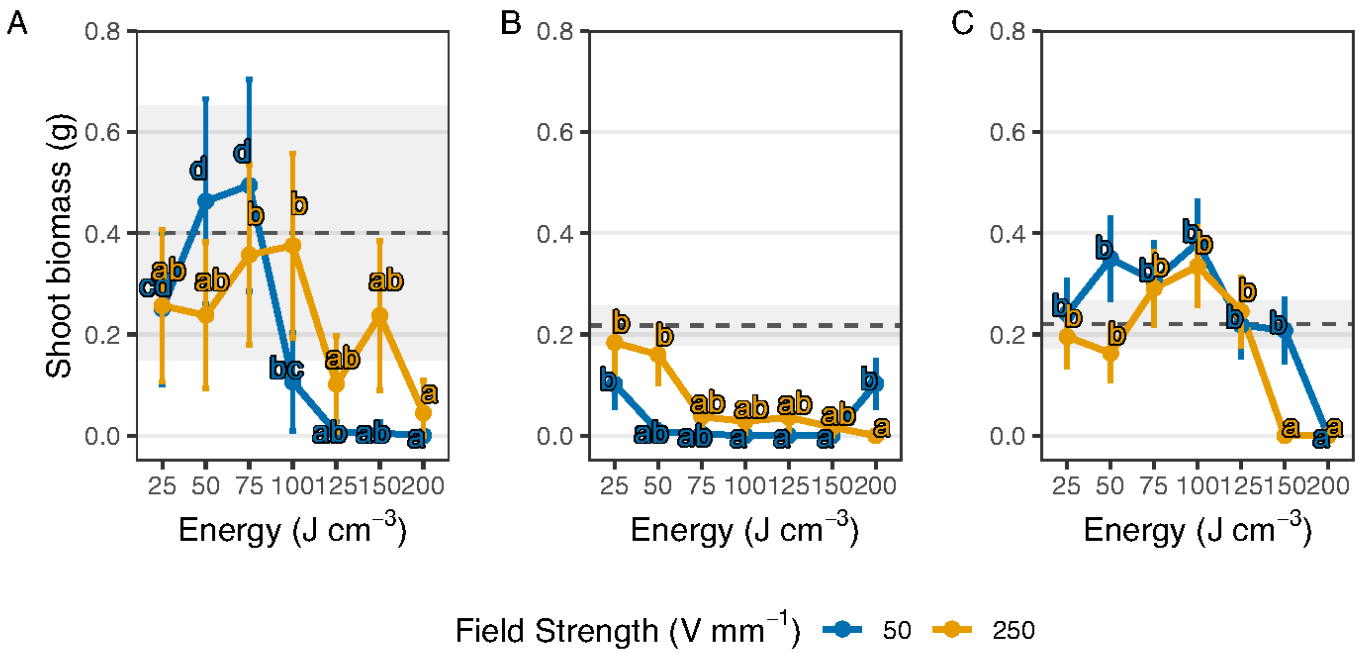

Figure 6

Shoot biomass of *Cyperus esculentus* (A), *Digitaria sanguinalis* (B), and *Echinochloa crus-galli* (C) after the application of pulsed electric field (PEF) using the parallel plate applicator. Propagules were treated with increasing energy densities (0–200 J cm⁻³) at two field strengths (50 and 250 V mm⁻¹). Different letters indicate significant differences among treatments according to Sidak's test ($p < 0.05$). Means and standard error of means ($n = 8$) are pooled from two studies. The dashed line and shaded area represent the mean and 95% confidence interval of the nontreated control.

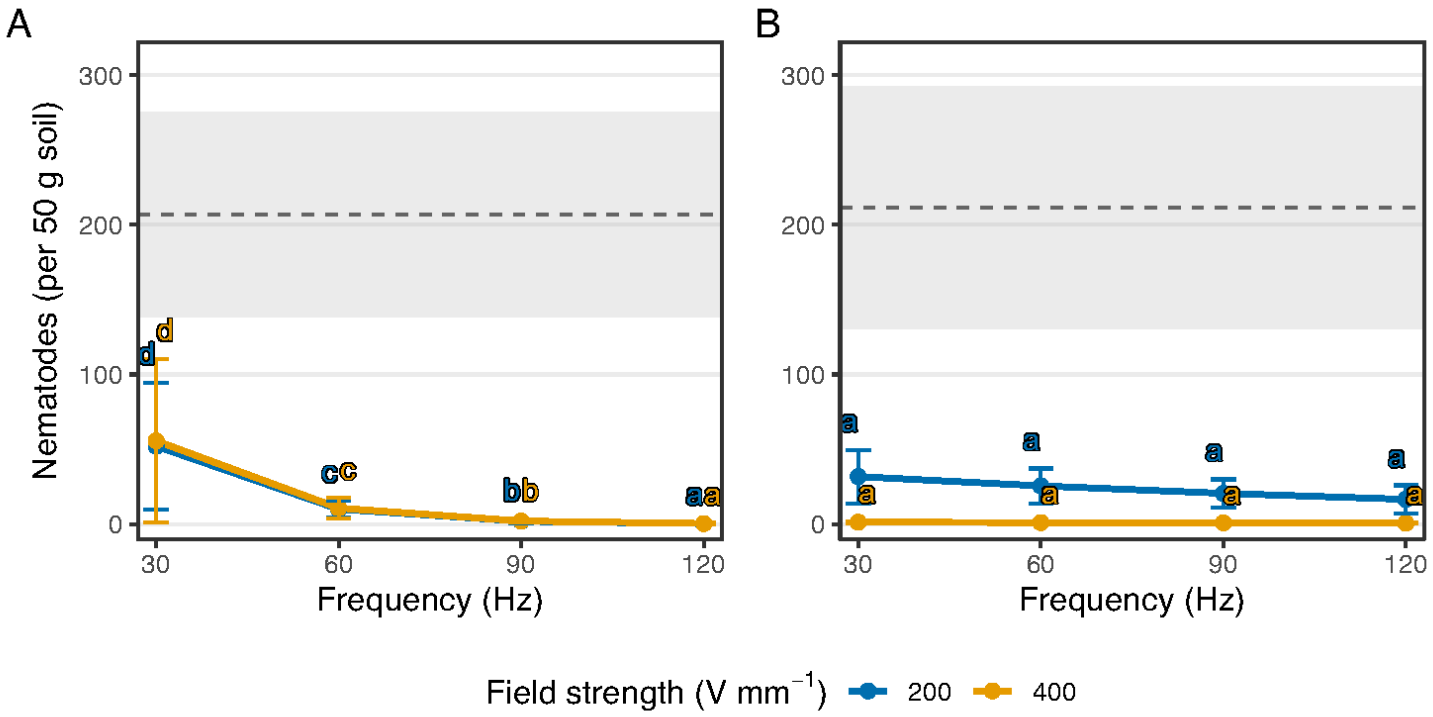

Figure 7

Response of *Meloidogyne chitwoodi* (A) and *Pratylenchus neglectus* (B) to pulsed electric field (PEF) treatments at varying field strengths (200 and 400 V mm⁻¹) and frequencies (0–120 Hz) using the parallel plate applicator. Different letters indicate significant differences among treatments according to Sidak's HSD test ($p < 0.05$). Means and standard error of means ($n = 8$) are pooled from two studies. The dashed line and shaded area represent the mean and 95% confidence interval of the nontreated control.

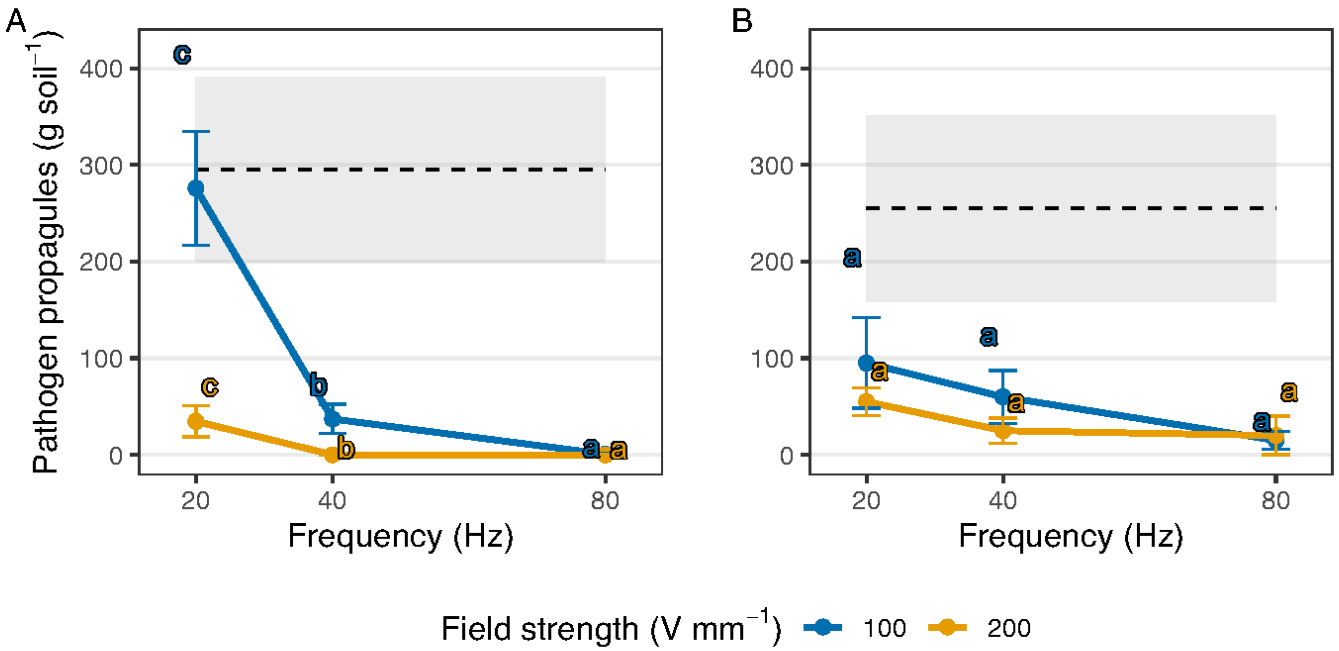

Figure 8

Response of *Phytophthora cinnamomi* (A) and *Phytophthora plurivora*(B) to pulsed electric field (PEF) treatments at varying field strengths (200 and 400 V mm⁻¹) and frequencies (0–120 Hz) using the parallel plate applicator. Different letters indicate significant differences among treatments according to Tukey's HSD test ($p < 0.05$). Means and standard error of means ($n = 8$) are pooled from two studies. The dashed line and shaded area represent the mean and 95% confidence interval of the nontreated control.

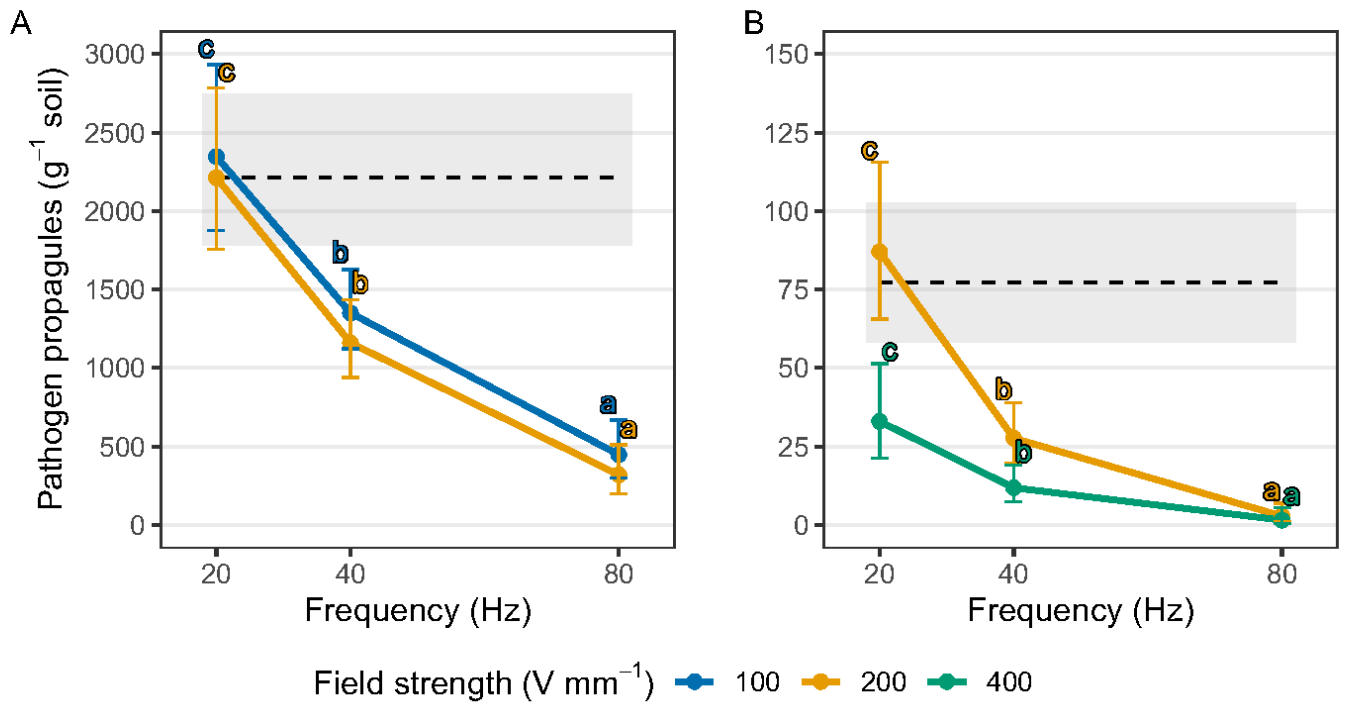

Figure 9

Response of *Verticillium dahliae* to pulsed electric field (PEF) treatments applied at field strengths of 100 and 200 (V mm^{-1}) (A) and 200 and 400 V mm^{-1} (B) with varying electrical frequencies (Hz) using the parallel plate applicator. Means and standard error of means (n = 8) are pooled from two studies. The dashed line and shaded area represent the mean and 95% confidence interval of the nontreated control.

Supplementary Files

This is a list of supplementary files associated with this preprint. Click to download.

- Supplementary.Sci.Rep.docx